Preferred citation: D.L. Taylor and J.K. Craver. Anisotropic elasticity of paper from sonic velocity measurements. In **Consolidation of the Paper Web**, *Trans. of the IIIrd Fund. Res. Symp. Cambridge, 1965*, (F. Bolam, ed.), pp 852–872, FRC, Manchester, 2018. DOI: 10.15376/frc.1965.2.852.

ANISOTROPIC ELASTICITY OF PAPER FROM SONIC VELOCITY MEASUREMENTS

D. L. TAYLOR, and J. K. CRAVER
Organic Chemicals Division, Monsanto Co., St Louis, U.S.A.

Synopsis—The theory of anisotropic elasticity for paper is reviewed. Sonic pulse velocity measurements were used to evaluate Young's modulus, shear modulus and Poisson's ratio of paper. The effects of fibre orientation and drying stresses on paper elasticity are readily measured by sonic velocity. A previously proposed relationship between the four in-plane elastic constants is approximately true for well-bonded paper. Local modulus variations in a single specimen can be detected by sonic velocity measurements. Any dependence of sonic velocity on substance is due to real differences in mechanical properties of the sheet.

Introduction

IN 1948, Hamburger reported the results of his study *The application of sonic techniques to the investigation of the effect of visco-elastic behaviour upon stress/strain relationships in certain high polymers,*[1] in which he described the use of a newly developed method for the evaluation of the elastic performance of textile fibres. The new technique involved the repeated generation of short-lived pulses of sound that were transmitted into the test filament. The time for the pulses to travel a known distance along the filament was accurately measured to yield a sonic velocity that was directly related to the instantaneous extensional elastic modulus (Young's modulus).

Hamburger was not the first to measure the speed of sound in synthetic fibres. In 1944, Ballou & Silverman[2] had refined an earlier crude approach of Myer & Lotmar[3] and succeeded in measuring sonic velocities in rayon, nylon and acetate yarns and in regenerated cellulose film. Their approach was to determine the wavelength of standing waves in the specimen, using a Rochelle salt piezoelectric crystal as an amplitude-sensing device. Continuous wave propagation techniques, however, have certain inherent shortcomings such as unwanted reflections due to end effects and minimum sample size dictated by the sample modulus itself (for a given input frequency). Hamburger circumvented such difficulties by simply pulsing the input signal.

Standing waves and interfering reflections were eliminated, because the acoustic energy of one pulse was dissipated before the succeeding pulse was generated. Sample lengths considerably less than a wavelength could be tested.

Hamburger used the sonic pulse propagation technique to measure the instantaneous elastic modulus of textile filaments during macroscopic straining to rupture. That portion of the total strain at any time caused by immediate elastic deformation was evaluated by an integration of the stress/modulus ratio up to the load in question. He was thus able to separate the immediate elastic component of the total strain in a specimen from the creep components.

In 1955, Chaikin & Chamberlain critically reviewed previous work on the dynamic elastic constants of textile materials[(4)] and indicated the advantages of pulse velocity techniques. They measured the dynamic elastic modulus of a large variety of fibres under conditions of varying tension and humidity.[(5)]

The pulse velocity technique was used by Charch & Moseley[(6)] to elucidate structure/property relationships in synthetic fibres. They showed that sonic velocity is nearly independent of degree of crystallinity in partly crystalline polymers at temperatures below their second-order transition point. The sonic velocity provided a sensitive measure of total molecular orientation in all polymers. Examination of homologous series of polyamides revealed significant correlations of sonic velocity with hydrogen bonding capacity of the polymers. In addition, the authors indicated several other areas for potential application of the sonic pulse technique. Later, Moseley examined in more detail the relationship between velocity and orientation and discussed the mechanism of sound propagation in oriented polymers.[(7)] The correlation of optical birefringence and sonic velocity methods for determining polymer orientation has been discussed.[(8–10)]

In spite of the successful application of sonic pulse velocity to the study of synthetic fibres over a period of almost two decades, this valuable technique has not, to our knowledge, been applied to paper. Dynamic mechanical testing, in general, has not been fully exploited in the paper industry. The few efforts that have been made are noteworthy. Van den Akker's recognition of the significance of dynamic measurement of paper physical properties almost 30 years ago[(11)] led to the development of a torsion device for flexural stiffness and internal viscosity determinations useful in paper softener work.[(12)] Horio & Onogi[(13)] measured the dynamic Young's modulus of many types of paper by the vibrating reed method and demonstrated the general utility of this technique in evaluating the effects of beating, humidity and sheet directionality. Sève & Perrin[(14)] have also applied the vibrating reed in studies of paper elasticity. The response of paper to low frequency sinusoidal strain of finite amplitude was the subject of an extensive study of Kubát, Nyborg & Steenberg.[15] Their measurements of dynamic modulus and internal friction demonstrated the pronounced strain hardening effects realisable in paper. In a recent paper, Rieman & Kurath[16] have examined the dynamic mechanical properties of paper as a function of relative humidity and dynamic strain amplitude, using a refined vibrating reed apparatus. Variations of the vibrating reed technique have been used by Steenberg[17] and by Nethercut[19] on paper and cellulose fibres.

We have chosen the sonic pulse velocity technique in our studies of paper elasticity for several reasons. In common with most dynamic mechanical test methods, it is non-destructive and insensitive to local sample variations ('weak spots'). In addition, the data are rapidly and easily obtained and are independent of sample dimensions. The velocity can be measured continuously while the specimen is undergoing change—either from external mechanical stresses or from attack by penetrating liquids. The major disadvantage of the pulse velocity method is that it is not well suited for measurement of the out-of-phase component of the complex Young's modulus. Thus, the damping or internal viscosity cannot be calculated. The vibrational frequency employed (10 000 c/sec is higher than that met in paper manufacture or use, but this is not of serious consequence, because the dynamic mechanical properties of paper and cellulose fibres are relatively independent of frequency.[13,19]

Our initial work in the area of sonic testing of paper[20] dealt broadly with the principles involved and basic applications. In the present paper, we briefly review the theory of anisotropic elasticity and present some of our recent findings on the elastic properties of paper.

Theory

DEFINE a rectangular co-ordinate system as shown in Fig. 1 with x_1 and x_2 (the machine- and cross-directions, respectively) and x_3 (the thickness normal to the plane of a paper sheet). In Fig. 1, an elemental cube of matter is shown with the nine possible stresses T_{ij} acting on each of three mutually perpendicular planes. Of course, a second set of stresses $-T_{ij}$ must act on the other three planes for mechanical equilibrium, but these are omitted for clarity. In the subscript notation, i refers to the direction of the stress and j refers to the plane on which the stress acts as defined by the direction of its normal. The T_{ij} with $i = j$ are ordinary tensile stresses and those with $i \neq j$ are shear stresses. The shear stresses occur in pairs (such as T_{12} and T_{21}), which must be equal in magnitude to produce the balanced couples necessary for mechanical equilibrium. Therefore, there are only six independent stresses possible—one shear and one tensile (or compression) acting in each direction. Any stress system can be resolved into these six components. Similarly, the deformation

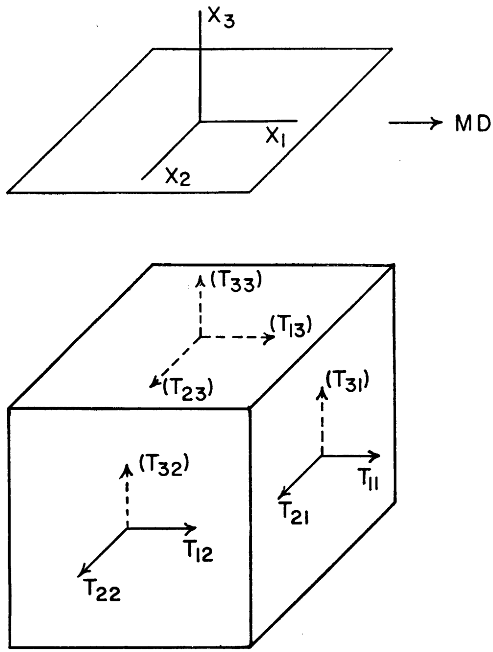

Fig. 1—Co-ordinate and stress system

or strain at any point in an elastic body can be resolved into six strain components S_{ij}. In a general anisotropic body, a stress can produce any of the six strains and a strain can be the result of any of the six stresses. If the body can be considered perfectly elastic, then stress and strain are proportional and a generalised Hooke's law applies—

$$T_{ij} = \sum_{k,l} b_{ijkl} S_{kl} \quad . \quad . \quad . \quad . \quad . \quad (1)$$

where the b coefficients are elastic moduli. The relationship can also be expressed inversely as—

$$S_{ij} = \sum_{k,l} s_{ijkl} T_{kl} \quad . \quad . \quad . \quad . \quad . \quad (2)$$

where the s coefficients are elastic compliances and have the units of reciprocal moduli.

In the sonic pulse technique as applied to films, the stresses involving the thickness direction are negligible or zero. These stresses are indicated by the dashed arrows in Fig. 1. Shifting to the contracted engineering notation[21, 24] (and with subscript changes of $11 = 1$; $22 = 2$; $12, 21 = 6$), equation (*1*) reduces in this case to—

$$\left.\begin{aligned} T_1 &= b_{11}S_1 + b_{12}S_2 + b_{16}S_6 \\ T_2 &= b_{21}S_1 + b_{22}S_2 + b_{26}S_6 \\ T_6 &= b_{61}S_1 + b_{62}S_2 + b_{66}S_6 \end{aligned}\right\} \quad . \quad . \quad . \quad (3)$$

For paper, we can assume biaxial symmetry of elastic properties in the plane of the sheet. In this case, shear stress is associated only with shear strain and vice versa[22] and equation (*3*) reduces further to—

$$\left.\begin{aligned} T_1 &= b_{11}S_1 + b_{12}S_2 \\ T_2 &= b_{12}S_1 + b_{22}S_2 \\ T_6 &= b_{66}S_6 \end{aligned}\right\} \quad . \quad . \quad . \quad . \quad (4)$$

The in-plane elastic properties of paper are therefore fully defined by four independent elastic constants, which are directly related to the velocity of propagation of sound waves in the plane of the sheet[20, 23]—

$$\left.\begin{aligned} b_{11} &= \rho c_1^2 \\ b_{22} &= \rho c_2^2 \\ b_{66} &= \rho c_s^2 \\ b_{12} &= \rho c_{12}^2 \end{aligned}\right\} \quad . \quad . \quad . \quad . \quad . \quad (5)$$

where ρ is the sample density, c_1 and c_2 are the longitudinal wave velocities in the x_1 and x_2 directions and c_s is the shear wave velocity, which is independent of direction in the plane of the sheet. The velocity c_{12} is not measured directly, but is a function of c_1, c_2, c_s and the phase velocity c_{45} at 45° to the principal axes[23]—

$$c_{12}^2 = (\tfrac{1}{2})[(4c_{45}^2 - c_1^2 - c_2^2 - 2c_s^2)^2 - (c_1^2 - c_2^2)^2]^{1/2} - c_s^2 \quad . \quad (6)$$

In sonic pulse propagation, the group or ray velocity is measured. This is the velocity with which the elastic energy of the mechanical wave is transmitted and is not necessarily equal (in magnitude or direction) to the velocity of propagation of the wave front (wave or phase velocity) in an anisotropic body. In the directions of symmetry (the machine- and cross-machine directions in paper), the phase and group velocities are equal and the first three parts of equation (*5*) apply directly, but, the phase velocity $c_{(45)}$ is not equal to the measured group velocity at 45°.[22] Hammack[23] has applied Musgrave's approach[22] to the case of planar films to derive $c_{(45)}$ from sonic group velocity measurements. A polar plot of group velocity against angle is first constructed. The velocity $c_{(45)}$ is then graphically evaluated as the radial distance to the tangent that is perpendicular to the 45° axis. Equation (*6*) then gives c_{12}^2, hence b_{12}.

The choice of density ρ in equation (*5*) defines the unit area to which the moduli b_{ij} refer. If ρ is chosen as the density of fibre substance, then b_{ij} refers to load per unit solid cross-sectional area.

The four elastic constants b_{11}, b_{22}, b_{12}, and b_{66} completely characterise the in-plane elastic behaviour of paper. They have the units of modulus (such as dyn/cm^2), but are *not* identical with commonly measured moduli, except for b_{66}. For example, Young's modulus is defined in terms of a single stress environment—

$$E_{11} = T_1/S_1 \quad . \quad . \quad . \quad . \quad . \quad (7)$$

but, from equation (*4*), we have—

$$E_{11} = b_{11} + b_{12}(S_2/S_1) \quad . \quad . \quad . \quad . \quad (8)$$

The familiar elastic constants—Young's modulus, shear modulus, Poisson's ratio—are all easily derived functions of the b_{ij} values, because they are simply related to the coefficients s_{ij} in the reciprocal form of equation (*4*)—

$$\left.\begin{aligned} S_1 &= s_{11}T_1 + s_{12}T_2 \\ S_2 &= s_{12}T_1 + s_{22}T_2 \\ S_6 &= s_{66}T_6 \end{aligned}\right\} \quad . \quad . \quad . \quad . \quad (9)$$

Thus, we have—

$$\left.\begin{aligned} E_{11} &= s_{11}^{-1} = (b_{11}b_{22} - b_{12}^2)/b_{22} \\ E_{22} &= s_{22}^{-1} = (b_{11}b_{22} - b_{12}^2)/b_{11} \\ \frac{E_{11}}{\nu_{12}} &= \frac{E_{22}}{\nu_{21}} = -s_{12}^{-1} = (b_{11}b_{22} - b_{12}^2)/b_{12} \\ G &= s_{66}^{-1} = b_{66} \end{aligned}\right\} \quad . \quad . \quad (10)$$

where ν_{ij} is Poisson's ratio for extension in the x_i direction and G is the in-plane shear modulus of elasticity.

For paper that is isotropic in the plane of the sheet such as laboratory handsheets, equation (*10*) simplifies to[20]—

$$\left.\begin{aligned} E &= \rho c^2(1-\nu^2) \\ \nu &= 1-(2c_s^2/c^2) \\ G &= \rho c_s^2 \end{aligned}\right\} \quad . \quad . \quad . \quad . \quad . \quad (11)$$

where c is the longitudinal wave velocity in the plane of the sheet. Because Poisson's ratio is ordinarily restricted to the range 0–$\frac{1}{2}$, the term $(1-\nu^2)$ will be between 0.75 and unity, usually about 0.90. For this reason, we refer to a *sonic modulus* $\tilde{E}$, defined as—

$$\tilde{E} = \rho c^2 \quad . \quad . \quad . \quad . \quad . \quad (12)$$

which does not require measurement of c_s and is a good approximation to the true Young's modulus. Similarly, the b_{ij} of equation (*5*) can also be termed sonic moduli in the anisotropic case.

The degree to which the sonic moduli approximate to the true Young's moduli is a function of the anisotropy and Poisson's ratio. If the fractional error Δ is defined as—

$$\Delta = (\tilde{E}-E)/E \qquad (13)$$

we have from equations (*5*), (*10*) and (*12*)—

$$\Delta = [(E_{11}/E_{22}\nu_{12}^{2})-1]^{-1} \qquad (14)$$

Table 1 outlines the range expected for Δ (which is the same in both principal directions).

TABLE 1—SONIC MODULUS APPROXIMATION FOR ANISOTROPIC PAPER

Modulus ratio, E_{11}/E_{22}	*Poisson's ratio,* ν_{12}	*Fractional error,* Δ
1.0	0.2	0.042
	0.4	0.190
2.0	0.2	0.020
	0.4	0.087
3.0	0.2	0.014
	0.4	0.056

From Table 1, we see that ordinarily equation (*12*) will result in an over-estimation of the true Young's modulus in the machine- and cross-direction by only 5–10 per cent. The modulus ratio calculated from the sonic modulus is exact, however, thus—

$$\tilde{E}_{11}/\tilde{E}_{22} = E_{11}/E_{22} \qquad (15)$$

Although the full in-plane elastic properties of paper are determined by the four elastic constants b_{ij} or s_{ij}, a plot of Young's modulus as a function of direction gives a more pictorial representation of the anisotropy. A transformation of the orthorhombic reduction of the general elasticity relations[33] gives—

$$1/E_{\theta} = \cos^4\theta/E_{11}+(1/G-2\nu/E)\sin^2\theta\cos^2\theta+\sin^4\theta/E_{22} \quad (16)$$

or equivalently—

$$1/E_{\theta} = s_{11}\cos^4\theta+(s_{66}+2s_{12})\sin^2\theta\cos^2\theta+s_{22}\sin^4\theta \qquad (17)$$

where E_{θ} is Young's modulus at angle θ to the x_1 direction.

Horio & Onogi found[13] that, when E_{θ} for paper is measured by the vibrating reed technique, the experimental results are described by the simpler relationship—

$$1/E_{\theta} = \cos^2\theta/E_{11}+\sin^2\theta/E_{22} \qquad (18)$$

or in terms of the compliance s_{ij}—

$$1/E_\theta = s_{11}\cos^2\theta + s_{22}\sin^2\theta \qquad (19)$$

Campbell[25] later pointed out that the empirical equation (*18*) is a special case of the exact relationship that is true if and only if—

$$1/G = 1/E_{11} + 1/E_{22} + 2\nu/E \qquad (20)$$

As indicated in our earlier paper,[20] the Campbell relationship of equation (*20*) is equivalent to—

$$s_{66} + 2s_{12} = s_{11} + s_{22} \qquad (21)$$

or

$$b_{66} + b_{12} = [b_{66}(b_{66} - b_{11} - b_{22}) + b_{11}b_{22}]^{1/2} - b_{66} \qquad (22)$$

If equation (*18*) is generally true of paper, then the special relationships expressed by equations (*20*)–(*22*) should have a basis in paper structure theory. Besides, from a practical viewpoint, the constant b_{12} would then be an analytical function of b_{11}, b_{22} and b_{66}, which are readily and directly measured by the pulse velocity technique.

Experimental

Instrumentation—The instrument employed throughout was one of commercial design[26] and was described in our earlier communication.[20] Briefly, a piezoelectric element resonant at about 10 kc is brought into contact with the paper test piece and is shocked into vibration parallel to the plane of the paper by a 5 μsec voltage pulse, which simultaneously activates a timing circuit. The mechanical wave travelling through a measured sample distance is detected by a second transducer whose output deactivates the timing circuit. The time of travel of the sonic pulse through the specimen is indicated directly on a recorder or meter. Distance spanned divided by travel time gives the sonic velocity.

Velocity polar diagrams—Paper test pieces roughly 5 in square were a convenient size for the determination of the angular dependence of sonic velocity. The velocity was measured at 15° intervals over a complete 180° sweep. Because commercial paper is orthogonally bisymmetric, a single 90° sweep between the principal axes should determine the entire angular dependence of velocity, but we have found that misalignment of as little as one degree between the assumed axes and the true axes of symmetry can be detected by the sonic velocity technique. We first plot sonic velocity against angle from the assumed machine-direction on tracing paper with rectangular co-ordinates. The exact location of the cross-direction is then identified by the position of a fold parallel to the velocity co-ordinate that produces good overlap of the two halves of the data set. The velocities are then plotted on one quadrant of polar co-ordinates, using the corrected true angle from the symmetry axis. The polar plots of velocity presented in this report have the two overlapping sets of data represented by different symbols.

Results and discussion

Oriented handsheets—The directional dependence of mechanical properties of paper results from two principal macroscopic factors—fibre orientation and external directional stresses during drying. Both factors should affect the velocity of sound in the plane of the sheet.

The sonic velocity in a natural cellulose fibre is probably much greater along the fibre axis than in the cross-fibre direction, considering the strong dependence of sonic velocity on total molecular orientation.(7) Fibre orientation in paper would contribute to an increased sonic velocity in the direction of orientation for this reason. Viewed at a microscopic level, the sound wave is propagated through the solid substance of the sheet only. The acoustical mismatch at fibre/air surfaces is too great to permit direct transmission of the sound through fibre and void space in series. Fibre orientation would reduce the actual sonic transmission path length in the direction of orientation, producing a decrease in transit time, hence an increase in the calculated velocity.

There is considerable evidence that external stresses during drying contribute greatly to sheet anisotropy,(27,28) partly as result of altered fibre mechanical properties.(29) The increased tensile strength of a papermaking fibre dried under tension is due to molecular orientation and stress redistribution in the fibre.(29) Both effects would be expected to increase the sonic velocity along the axis of a fibre, hence increase the velocity through a sheet dried under strain.

The effects of fibre orientation and drying stresses on sheet anisotropy were determined by the sonic velocity technique on laboratory handsheets. A bleached kraft softwood pulp (500 CSF) was formed into handsheets of varying degree of fibre orientation on a specially designed sheetmaking apparatus.(30,31) The wet sheets were then air-dried under various dimensional constraints.

The velocity polar diagrams for sheets of similar degrees of fibre orientation are shown in Fig. 2–4. The inner circle in these diagrams is the shear wave velocity. In Fig. 2, we have plotted the velocity diagram for the oriented handsheet dried in a frame that prevented shrinkage in all directions (biaxial constraint). The velocity profile in this case reflects the fibre orientation directly. A significant aspect of Fig. 2 is that the maximum velocity is found at 20° from the machine-direction. The data of Prusas(30) on fibre orientation, shrinkage and hygroexpansivity for other oriented handsheets formed on the same sheetmaking machine exhibit a similar maximum (or minimum) at about 15°. This gives strong support to our claim that, in the absence of non-uniform drying stresses, the sonic velocity profile of Fig. 2 is directly due to fibre orientation.

A wet web of similar fibre orientation was dried under machine-direction constraint. The resulting velocity polar diagram is shown in Fig. 3. The maximum velocity is now greater than before and is located in the machine-direction. The cross-direction velocity has been reduced. The velocity

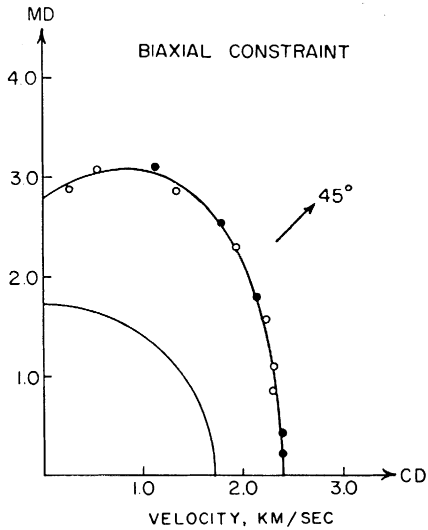

Fig. 2—Fibre oriented handsheet—biaxial drying constraint

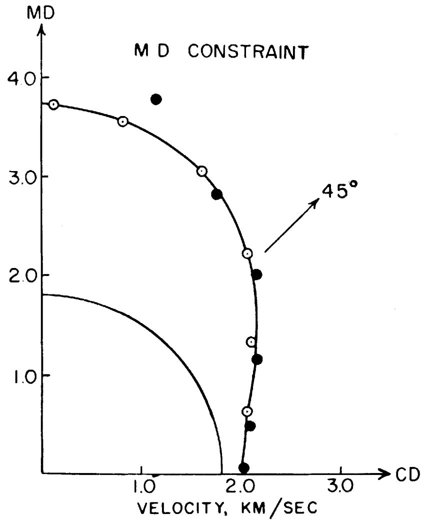

Fig. 3—Fibre oriented handsheet—machine-direction drying constraint

anisotropy of this sample is typical of commercial papers. Here, the mechanical anisotropy results from a combination of fibre orientation and drying stress effects.

A third wet web of similar fibre orientation was dried under cross-direction constraint with freedom to shrink in the machine-direction. This is a condition not met on commercial papermachines. The resulting velocity profile is shown in Fig. 4. The maximum velocity is now close to the cross-direction. The cross-direction drying stress has succeeded in masking the effects of fibre orientation.

Fig. 2–4 are superimposed in Fig. 5 for direct comparison of the effects of fibre orientation and directional stress during drying. The velocities in the principal directions as well as the shear wave velocities are summarised in Table 2. The shear wave velocity is unaffected by drying stresses.

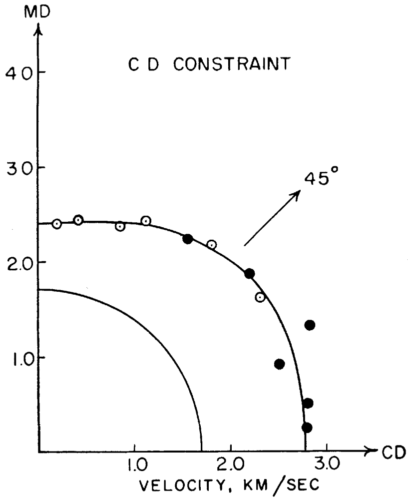

Fig. 4—Fibre oriented handsheet—cross-direction drying constraint

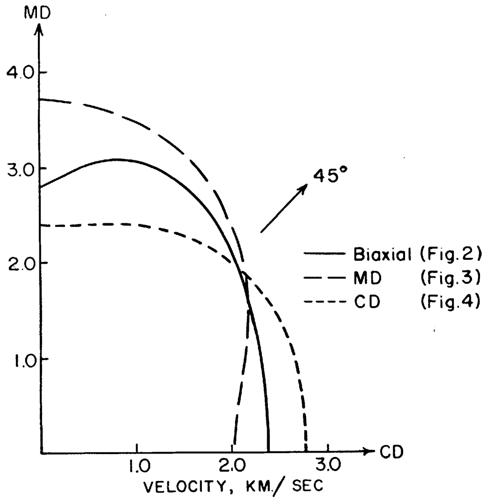

Fig. 5—Fibre oriented handsheets—effect of drying constraints

TABLE 2—EFFECT OF DRYING STRESS ON SONIC VELOCITY

Drying condition	*Sonic velocity, km/sec*			*Modulus ratio, equation (15)*
	MD	*CD*	*Shear*	
Biaxial constraint	2.80	2.41	1.72	1.35
MD constraint	3.73	2.02	1.81	3.40
CD constraint	2.40	2.80	1.71	0.74

Modulus anisotropy—As discussed earlier, there is some evidence[13, 20, 25] that paper exhibits a special relationship between its in-plane elastic constants that is not contained in classical elasticity theory. We have examined this point further by the sonic pulse velocity technique, which we believe provides the most reliable measure of the required elastic constants. On the basis of recent investigations, we have modified our earlier conclusion[20] and now consider that the special relationship expressed by equations *(20)*–*(22)* is only approximately true for many well-bonded papers. Velocity data sufficient for the complete evaluation of the in-plane elastic constants were obtained on a strong unbleached kraft wrapping paper, a bleached sulphite writing paper, a low density filter paper and a 100 per cent synthetic fibre paper (polyacrylonitrile). The velocity data and modulus anisotropy diagrams are presented in Fig. 6–13. The inner circle on each of the figures gives the value of the shear

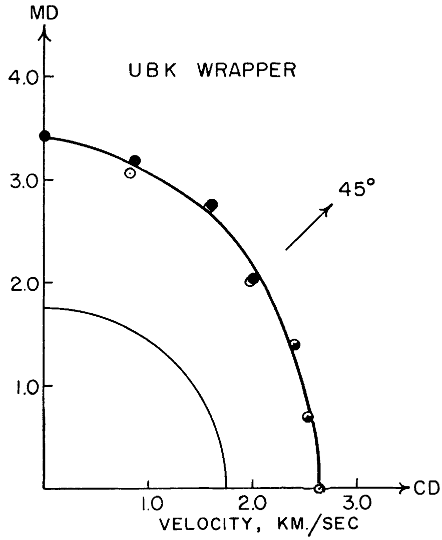

Fig. 6—Unbleached kraft wrapping paper—velocity profile

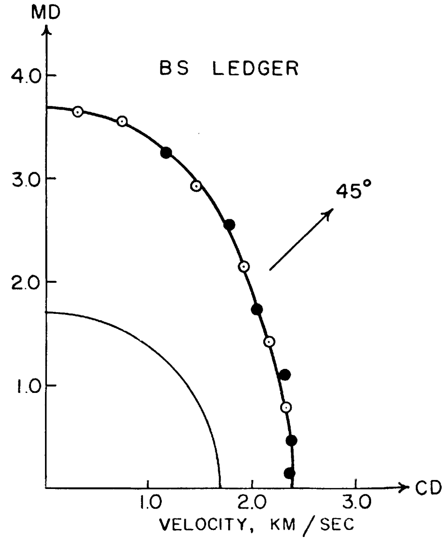

Fig. 7—Bleached sulphite ledger paper—velocity profile

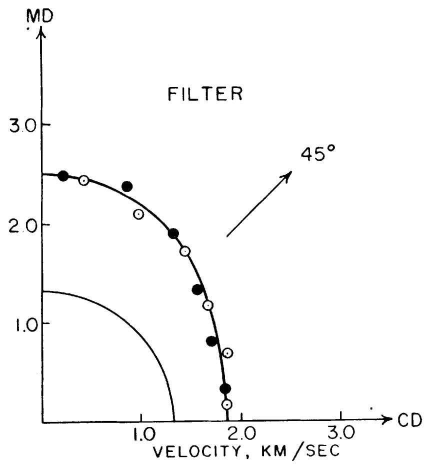

Fig. 8—Filter paper—velocity profile

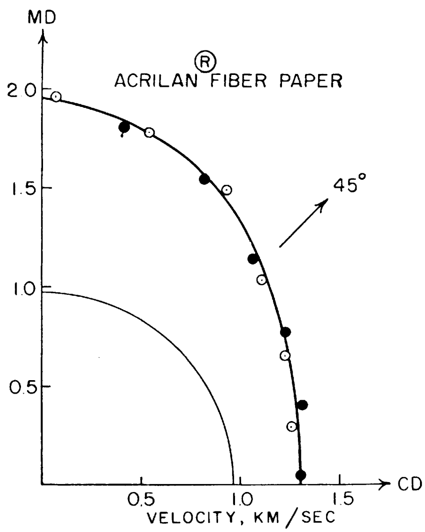

Fig. 9—Synthetic fibre paper—velocity profile

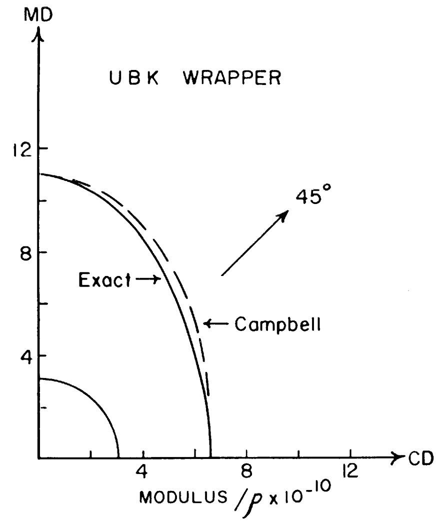

Fig. 10—Unbleached kraft wrapping paper—modulus anisotropy

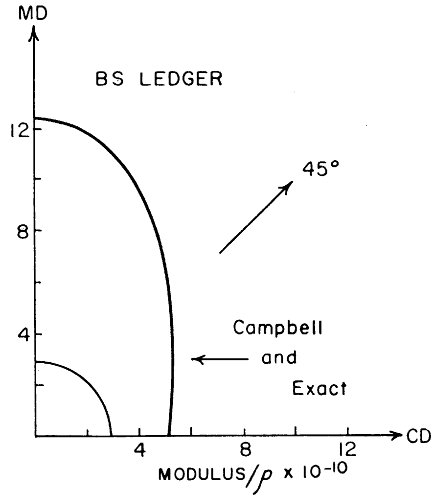

Fig. 11—Bleached sulphite ledger paper—modulus anisotropy

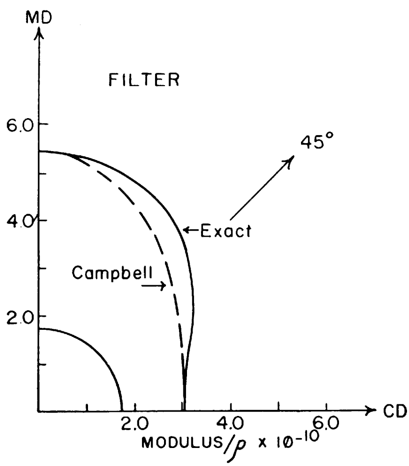

Fig. 12—Filter paper—modulus anisotropy

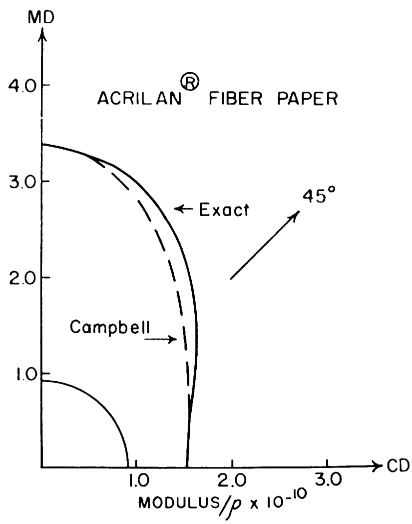

Fig. 13—Acrylic fibre paper—modulus anisotropy

velocity and shear modulus, which are independent of direction in the plane of the sheet.

The overlap of velocity data for each sample (filled and open circles) is quite satisfactory. All four of the samples are therefore accurately symmetrical about the directions of maximum and minimum velocity, which, in turn, are mutually perpendicular. The samples are therefore typical machine-made fibre webs.

In each of the modulus anisotropy diagrams, the curve labelled *Exact* was calculated according to equation (*17*) and that labelled *Campbell* was calculated from equation (*19*). The moduli are all expressed in units of dyn/cm^2, which result when the velocities are expressed in cm/sec and the density in g/cm^3. For convenience, the modulus/density ratio is employed throughout, so that only velocity measurements are involved.

The two methods of calculating E_θ result in the same value at $\theta = 0°$ and 90° as is evident from equations (*17*) and (*19*). The Campbell relationship approximates the exact relationship for the kraft paper. The agreement is perfect for the sulphite writing paper, but quite poor in the case of the filter paper. The agreement is intermediate for the acrylic fibre* paper.

A check was made of reproducibility in the sonic determination of the elastic compliances s_{ij}. Three samples of the unbleached kraft paper representing adjacent areas on a large sheet were tested. The entire experimental and analytical procedure for determining s_{ij} was carried out on each sample. The coefficient of variation for single determinations of s_{11}, s_{22} and s_{66} was 2 per cent, whereas that for s_{12} (which involves the graphical evaluation step) was 7 per cent.

We conclude from these data on modulus anisotropy in machine-made paper that the special relationship between the elastic constants expressed by equations (*20*)–(*22*) is approximately true for typical well-bonded paper.

Contour diagrams—The non-destructive nature of the sonic velocity test for elasticity permits the mapping of local modulus variations in a single test piece of paper. To our knowledge, this has never before been done. We present two examples of such mapping.

An 8 in × 8 in handsheet was formed on a Noble and Wood laboratory sheetmaking machine in the usual manner. A square grid was laid out on the sample with a 2.5 cm spacing. The two probes of the sonic pulse propagation apparatus were set at a fixed distance of 5.0 cm apart and the transit time was measured for 5 cm parallel paths centred over each of the grid intersection points. The transit times were rounded to the nearest scale unit and recorded

* Acrylic fibres referred to are Acrilan

at the grid points. Contour lines of constant transit time (constant velocity or modulus) were then sketched in as shown in Fig. 14.

The data of Fig. 14 are quite reproducible and only minor changes in the contour pattern result when replicate sets of transit times are obtained. The contours probably represent the effect of flow patterns that existed in the fibre slurry at the time of sheet formation.

Code	2	4	6	8
Velocity, km/sec	2.78	2.63	2.50	2.38

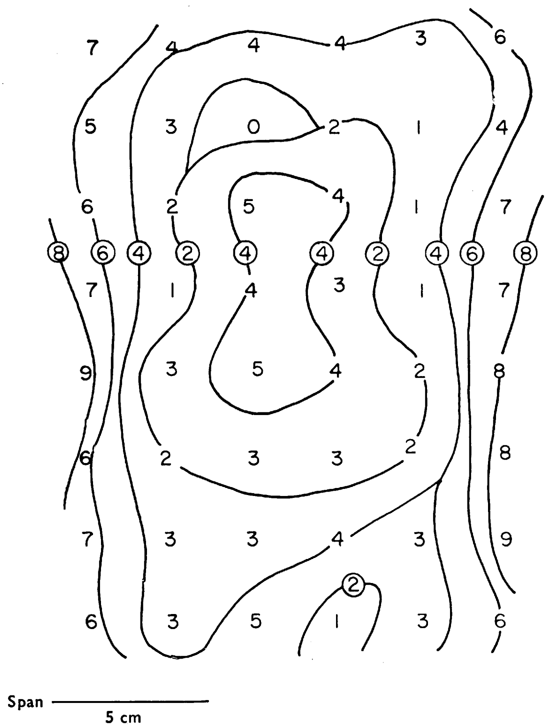

Fig. 14—Handsheet velocity contour map

The same procedure was carried out on a commercial machine-made sheet, except that three velocities were measured at each grid point—the longitudinal wave velocities in the machine-direction and cross-direction (c_1 and c_2) and the shear wave velocity c_s. The resulting contour patterns for c_1, c_2 and c_3 are presented in Fig. 15–17. Although the details vary, there are striking similarities in the three diagrams. The contour lines run generally in the machine-direction (unlike the circular pattern for the handsheet) and produce the steepest gradient at the sides and a plateau or saddle near the centre. A significant observation is that the range of values for the three modes of propagation are roughly the same and the high values of each are found in about the same region of the sheet. Thus, the contour lines cannot be

Code	3	5	7	9
Velocity, km/sec	3.55	3.33	3.14	2.98

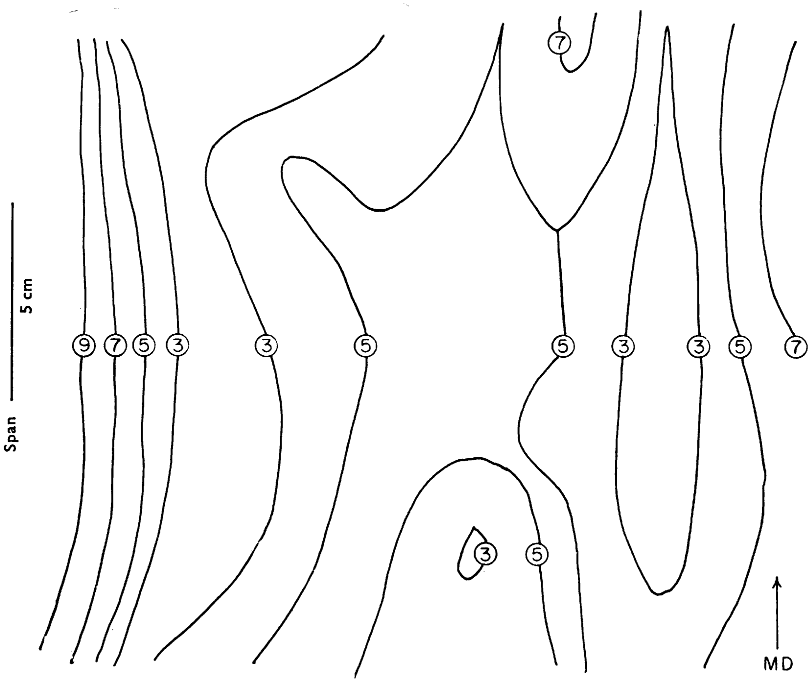

Fig. 15—Machine paper machine-direction velocity contour map

the result of fibre orientation or drying stress patterns, because these would produce a minimum c_2 where c_1 is maximum. Possibly, local variations in wet pressure, drying temperature or drying rates are the source of the modulus contours.

Effect of substance—A major advantage of sonic velocity evaluation of paper elasticity is that the velocity is independent of sample dimensions, including thickness, but we have found[20] that the sonic velocity in handsheets does depend on substance (or thickness) in the range below 60 g/m^2.

A bleached sulphite pulp beaten to 500 CSF was formed into handsheets of various substances on a Noble and Wood laboratory sheetmaking machine. The load/elongation curves were determined on an Instron tester and the longitudinal sonic wave velocities were measured. The results are presented in Table 3.

Code	2	4	6	8	10
Velocity, km/sec	2.49	2.36	2.27	2.18	2.09

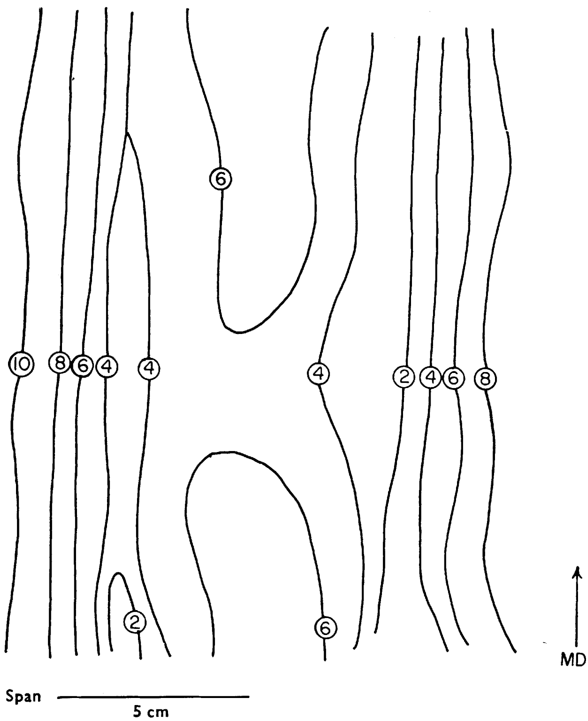

Fig. 16—Machine paper cross-direction velocity contour map

The measured values of ultimate tensile strength and initial tensile strength slope were multiplied by the ratio (60/substance) to 'correct' them to a common substance of 60 g/m^2. The corrected tensile strength parameters and the sonic velocity all increase with sheet substance up to about 60 g/m^2, then become independent of substance. The dependence of velocity on substance therefore is due to real differences in the elastic properties of the sheets.

In a similar experiment, a beaten (500 CSF) bleached kraft softwood pulp was formed into sheets of various substances before and after removal of the

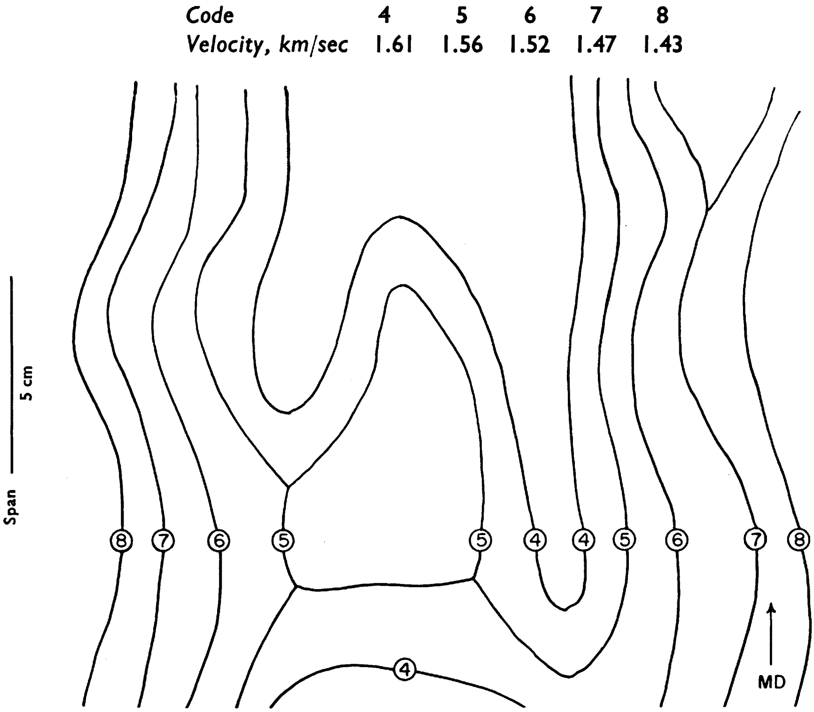

Fig. 17—Machine paper shear velocity contour map

TABLE 3—SUBSTANCE DEPENDENCE OF TENSILE AND SONIC PROPERTIES OF HANDSHEETS

Substance, g/m²	*Ultimate tensile strength, lb/in*		*Tensile strength slope, lb/in per cent*		*Sonic velocity, km/sec*
	Measured	*Corrected*	*Measured*	*Corrected*	
7.5	0.41	3.3	0.30	2.37	1.18
12.0	1.06	6.8	0.76	3.80	1.49
15.5	1.68	6.5	1.44	5.59	1.51
20.5	3.20	9.4	2.27	6.65	1.90
26.5	5.60	12.7	3.40	7.70	1.91
39.0	9.50	14.6	5.66	8.70	2.35
66.0	23.3	21.2	11.4	10.4	2.42
90.5	35.3	23.4	15.2	10.1	2.42
119.5	46.2	23.2	19.5	9.8	2.48

fines through a 100 mesh screen. The thickness and longitudinal and shear wave velocities were measured. The sonic velocities for both whole and classified woodpulp were independent of substance in the region above

TABLE 4—EFFECT OF SUBSTANCE AND CLASSIFICATION ON SONIC VELOCITIES IN HANDSHEETS

Pulp used	*Substance, g/m²*	*Sonic velocity, km/sec*		*Apparent density, g/cm³*
		C, Longitudinal	*Cs, Shear*	
Woodpulp (whole)	69.0	3.03	1.67	0.502
	92.5	2.98	1.85	0.570
	115.	3.23	1.86	0.607
	136.	3.14	1.86	0.645
		Average 3.10	1.81	
Classified woodpulp	68.8	2.89	1.67	0.484
	94.0	2.94	1.73	0.545
	112.	2.84	1.70	0.575
	132.	2.87	1.74	0.597
		Average 2.88	1.71	

60 g/m² as for the sulphite pulp. The data for the high substance region is summarised in Table 4.

The apparent densities recorded in Table 4 were calculated from the substance and measured thickness of single sheets (using a standard paper caliper at loading pressures of about 8 lb/in²). The increase of apparent density with substance is related to the surface roughness of handsheets made on a Noble and Wood machine[(32)] and does not indicate a change in the true density of the interior substance of the handsheets. The substance/thickness relationship for these handsheets was linear in this high region of substance and the slope of the relationship gives a bulk density that more faithfully represents the sheet structure[(32)] as attested by the constancy of the sonic velocities. The elastic moduli and Poisson's ratio calculated from the averaged velocities by equation *(11)* are summarised in Table 5. The 'true' apparent density is that obtained from the substance/thickness slope.

TABLE 5—ELASTIC CONSTANTS OF HANDSHEETS (from Table 4)

Property	*Pulp: bleached kraft, 500* CSF	
	Whole	*Classified*
Young's modulus, $E/\rho \times 10^{-10}$	8.65	7.59
Shear modulus, $G/\rho \times 10^{-10}$	3.28	2.93
Poisson ratio, ν	0.32	0.30
True apparent density, g/cm³	0.926	0.870

Pulp classification reduces the sheet's strength parameters and the density somewhat as has been noted before.[(34)] The calculation of Poisson's ratio is quite sensitive to experimental errors, because of the squaring of both measured velocities as seen in equation (*11*). The Poisson ratios of about 0.3 actually obtained are reasonable.[35] This fact alone contributes considerably to our confidence that the sonic wave propagation equations derived for homogeneous media can be applied to paper.

Conclusions

MEASUREMENT of the velocity of sound in paper yields complete information on the in-plane elastic properties including Young's modulus, the shear modulus and Poisson's ratio. The equations relating sonic velocities to elastic constants, valid for homogeneous media, are applicable to paper in spite of its heterogeneous, porous nature. The velocity of sound in paper is dependent on fibre orientation, the degree of interfibre bonding and the elastic properties of the fibres themselves. The local variations of elastic properties in single sheets of commercial or handmade paper can be readily mapped by sonic velocity measurements.

References

1. Hamburger, W. J., *Textile Res. J.*, 1948, **18** (12), 705–743
2. Ballou, J. W. and Silverman, S., *Textile Res. J.*, 1944, **14** (9), 282–292
3. Meyer, K. H. and Lotmar, W., *Helv. Chim. Acta.*, 1936, **19** (1), 68–86
4. Chaikin, M. and Chamberlain, N. H., *J. Textile Inst.*, 1955, **46** (1), T25–T43
5. Chaikin, M. and Chamberlain, N. H., *J. Textile Inst.*, 1955, **46** (1), T44–T62
6. Charch, W. H. and Moseley, W. W., *Textile Res. J.*, 1959, **29** (7), 525–535
7. Moseley, W. W., *J. appl. Polymer. Sci.*, 1960, **3** (9), 266–276
8. Morgan, H. M., *Textile Res. J.*, 1962, **32** (10), 866–868
9. Ward, I. M., *Textile Res. J.*, 1964, **34** (9), 806–807
10. Ross, S. E., *Textile Res. J.*, 1964, **34** (7), 565–571
11. Van den Akker, J. A., *Mechanics, Hydraulics, Heat and Thermodynamics*, (Institute of Paper Chemistry, Appleton, Wis. 1937), 84–86
12. McPherson, W. H. Jnr., *Tappi*, 1950, **33** (11), 531–537
13. Horio, M. and Onogi, S., *J. appl. Phys.*, 1951, **22** (7), 971–977
14. Sève, R. and Perrin, H., *ATIP Bull.*, 1954, (1), 1–7
15. Kubát, J. Nyborg, L. and Steenberg, B., *Svensk Papperstidn.*, 1963, **66** (19), 754–764
16. Riemen, W. P. and Kurath, S. F., *Tappi*, 1964, **47** (10), 629–635
17. Steenberg, B., *Finnish Paper & Timber J.*, 1947, **29** (7a), 64
18. Nethercut, P. E., *Tappi*, 1957, **40** (1), 39–44
19. Fujino, K., Kawai, H. and Horino, T., *Textile Res. J.*, 1955, **25** (8), 722–737
20. Craver, J. K. and Taylor, D. K. *Tappi*, 1965, **48** (3), 142–147
21. Condon, E. V. and Odishaw, H., Editors, *Handbook of Physics* (McGraw-Hill Book Co., New York, 1958), pt. 3, 11
22. Musgrave, M. J. P., *Proc. Royal Soc.*, 1954, **A226** (1166), 356–366

23. Hammack, T., Dept. Mech. Eng., MIT, Cambridge, Mass., 1963, unpublished work
24. Hearmon, R. F. S., *Applied Anisotropic Elasticity* (Oxford University Press, London, 1961)
25. Campbell, J. G., *Austral. J. appl. Sci.*, 1961, **12** (3), 356–357
26. H. M. Morgan Co. Inc., Cambridge, Mass., Original design S. R. Rich, U.S. Patent 2 706 906 (26th April 1955)
27. Edge, S. R. H., *Chem. & Ind.*, 1948, **67** (12), 803–807
28. Schultz, J. H., *Tappi*, 1961, **44** (10), 736–744
29. Jentzen, C. A., *Tappi*, 1964, **47** (7), 412–418
30. Prusas, Z. C., *Tappi*, 1963, **46** (5), 325–330
31. The assistance of The Mead Corporation, Chillicothe, Ohio, in providing the use of their equipment and time is gratefully acknowledged
32. Taylor, D. L., *Tappi*, 1964, **47** (7), 165A–167A
33. Hearmon, R. F. S., *Mechanical Properties of Wood and Paper*, Ed. R. Meredith (North-Holland Publishing Co., Amsterdam, 1953), Chapter 2
34. Thode, E. F. and Ingmanson, W. L., *Tappi*, 1959, **42** (1), 74–83
35. Kallmes, O. J., Stockel, I. H. and Bernier, G. A., *Pulp & Paper Mag. Can.*, 1963, **64** (10), T449–T456

Discussion

Dr H. K. Corte—I have one question concerning the technique. As I understand it, when you place a probe more or less loosely on to the surface of the paper, you must surely move the paper sideways. How do you make certain that the friction between the probe and the paper is large enough to move the paper?

Dr D. L. Taylor—For the measurements in the paper, the specimens were lying flat on a sound-adsorbing rubber pad so that the probes rested on the paper. Transmission of the vibration into the paper was no problem. The probe rides only on the surface and moves the whole sheet through its full thickness. In the normal substance range, there is no difference on turning the sheet around; as soon as a thick caliper is reached, there is a difference.

Dr D. Wahren—You put a square pulse into the paper. What does the transmitted pulse look like and can the transfer function tell us something about the standard deviation of different pads through the sheet or about their relationship in the elastic moduli?

Dr Taylor—No, we do not put a square pulse in the sheet and therefore that information is not available. The sending crystal is actually shocked into vibration, but does not resonate at constant amplitude for any length of time.

Dr Corte—You demonstrate in one graph the so-called integrating nature of this technique and the sample you showed, simplified, had regions of high elastic modulus and low elastic modulus in series. This is one of the two possible models for heterophase materials, but what happens when these two regions are in parallel?

Dr Taylor—The sonic velocity measured would be the speed of sound through the higher modulus material, because the slower pulse would arrive too late for the timing circuit to sense it.

Dr J. Kubát—It may be mentioned here that the in-plane shear modulus of paper can easily be determined by the torsion pendulum technique. In agreement with the results being presented, we found in our measurements with this method that the shear modulus is independent of the sheet anisotropy—that is, it remains fairly constant when the orientation of the sample is varied.*

Mr A. P. Taylor—What is the smallest distance between the probes measured and what is the influence on accuracy?

Dr Taylor—This depends of course on the physical size of the probes, which I imagine could be constructed differently. With the present construction, this smallest distance is about 1.5 cm. The question of accuracy comes down to the following. Apart from the delay in the signal that the sample produces (which you want to measure), there is an inherent delay in the electrical system of the instrument. At such small distances, this inherent delay starts to become of appreciable relative size and would reduce your accuracy for that reason.

Dr Corte—You said that in the parallel model you would measure the elastic modulus of the stiffer material. This is different, of course, from what you would measure in the tensile tester, because there a modulus is measured that is given by $1/E = 1/E_1 + 1/E_2 + \dots$ What we have are parallel regions of lower and higher modulus, so this would mean that the regions of lower modulus (the thin spots in the paper) would be suppressed and you would find too high a modulus.

Dr Taylor—This depends upon whether the region of low modulus is in the direct path of the signal or not; in other words, the signal has to get from the sending transducer to the receiving transducer and, if this low modulus region exists across the whole width of the sample, then obviously the sound wave has to get through it to reach the other transducer. If this is a relatively small region somewhere in the sonic path, then the signal picked up may refer to the wave that has gone around this low modulus region.

* Kubát, J. and Lindbergson, B., *Svensk Papperstidn.*, 1965, **68** (21), 743–756